Energieforschungsprogramm

Publizierbarer Endbericht

Programmsteuerung:
Klima- und Energiefonds

Programmabwicklung:
Österreichische Forschungsförderungsgesellschaft mbH (FFG)

Endbericht
erstellt am
30/03/2023

Projekttitel: SorSens

Projektnummer: 881187

Ausschreibung	6. Ausschreibung Energieforschungsprogramm
Projektstart	01/07/2021
Projektende	31/12/2022
Gesamtprojektdauer (in Monaten)	18 Monate
ProjektnehmerIn (Institution)	FH-OÖ F&E GmbH
AnsprechpartnerIn	Bernhard Zettl
Postadresse	4600 Wels, Stelzhamerstr. 26
Telefon	+43 050 804 46918
Fax	
E-mail	Bernhard.zettl@fh-wels.at
Website	ASiC - FH OOE (fh-ooe.at)

SorSens

DEVELOPMENT OF A VIRTUAL SENSOR FOR STATE-OF-CHARGE EVALUATION OF TCM-ENERGY STORAGE

Authors
Bernhard Zettl
Michael Reisenbichler
Harald Kirchsteiger
Nayrana Daborer-Prado
Florian Wörl
Waldemar Wagner
Gayaneh Issayan

1 Content

2 Introduction

Thermal energy storages (TES) are believed to be appropriate candidates to play an important role in the future thermal management system. Broad deployment of energy storage technologies for an increased share of renewable energy is motivated by global climate action and the ambition of CO2 reduction.

The ability of thermochemical materials (TCM) to store energy long-term with practically no losses during the conservation phase makes them promising candidates for seasonal storage applications. High energy densities using the zeolite-water couple have been demonstrated for some applications, exceeding those of water storage by a factor of 2-3 (Hauer, 2020) (Zettl, 2020). There are several process solutions for sorption technology, open and closed systems, as well as moving-bed and fixed-bed reactions, which have specific advantages.

For all types of energy storage, the current state of charge (SOC) is an important parameter for operation and control. In contrast to sensible heat storage, the state of charge of thermochemical storage cannot be determined via the current discharge temperature. Rather, the current moisture content of the material and the moisture distribution over the entire storage system is a representative value for the state of charge. Since the material moisture balance is much more difficult to measure with “inline” methods (without taking probes) than the temperature, various physical measurement methods were tested in a preliminary project. One of the best ways is to utilize the dielectric conductivity, or permittivity, which correlates with the moisture content of the material. It can be detected, for example, by utilizing microwaves or by determining electrical capacitance (Zettl, 2022). However, the moisture measurement methods react sensitively to density fluctuations and temperature differences in the material, therefore comprehensive error correction and the combination of different measurement methods can improve accuracy here. For this purpose, a virtual sensor is being developed that eliminates various factors that interfere with the measurement and significantly increases the measurement quality.

3 Methodology

3.1 Sensor architecture

There are currently no sensors available for directly measuring the state of charge of sorption materials storage systems. An indirect method relying on electrical capacitance measurement was shown to be feasible in a laboratory environment (Kirchsteiger and Kefer, 2020). However, the method suffers from calibration requirements which potentially restrict practical applications: Material density fluctuations in moving bed applications and temperature influences the signals widely. SOC determination can be significantly enhanced by combining hardware sensors with appropriate mathematical models for so-called virtual sensors.

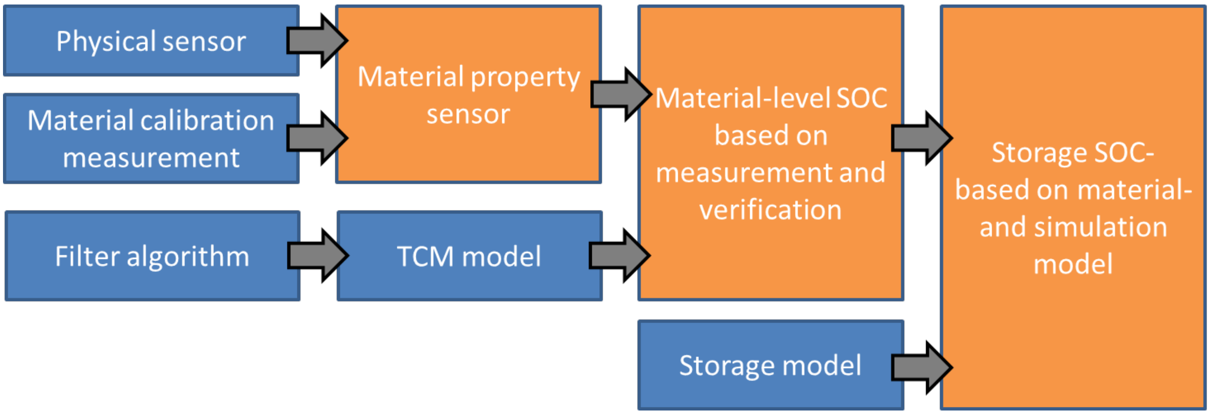

Figure 1: Principle of the operating levels of the virtual sensor

From a systems-theory point of view, the SOC of the sorption storage is an internal state which is not accessible for direct measurement (orange elements in Figure 1). There is the possibility to estimate this internal state using sophisticated software tools such as dynamic state observers. A particular type of observer, known as Kalman-filter, is implemented to take advantage of a combined model-based and real-time measurement strategy. Appropriately tuned, the filter assures a balanced SOC estimate which is not directly affected by short-time measurement errors (for example: temporary drops in a temperature measurement) since they are not plausible compared to the implemented model. At the same time, inevitable systematic model deviations are compensated with the aid of real-time measurements.

3.2 Adsorption model: Open system

The material adsorption model used in this work represents a sorption storage system of a zeolite bed. An axial humid airflow or vapor diffusion drives the sorption process and allows direct charging/discharging of the sorption material. The model implementation is done in Simulink, an additional package of MATLAB. To perform the numerical simulations, the model is based on the following assumptions (Daborer-Prado, et al., 2019):

- a one-dimensional approach is assumed, where no radial influence is considered
- a lumped element storage model is used for material and airflow, it is assumed that the air leaves each store node with the node temperature
- the sorption equilibrium is modelled by the Dubinin-Astakhov-approach and the reaction kinetics is described by a linear driving force approach
- the specific heat capacity of the air is not a function of the humidity or the temperature in the system; the specific heat capacity of the solid is only a function of humidity (water loading) but not of the temperature in the system.

3.3 Adsorption model: Closed System

According to the experimental investigations (see next chapter), the development of the numerical model for the closed sorption system was focused on a fixed bed reactor with zeolite 13XBF as sorption material.
A literature review was conducted to collect possible modeling approaches for sorption storage systems and the corresponding mathematical descriptions of the main components (e.g., adsorber/reactor, evaporator/condenser) and the governing physical processes (e.g., sorption equilibrium correlations). Figure 2 shows the energy balance equation for the sorption material (adsorbent) during the adsorption process in the adsorber/reactor.

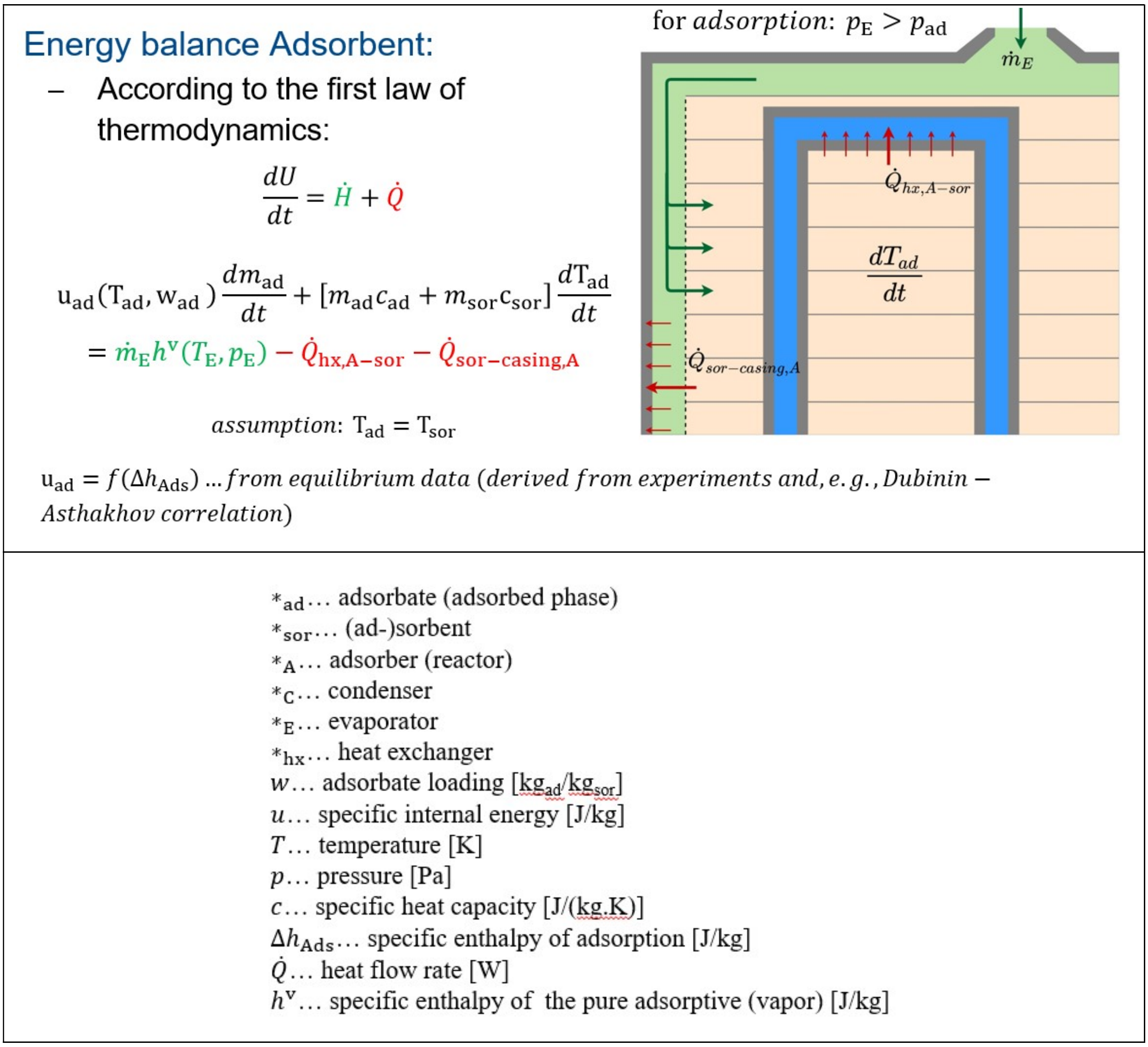

Energy balance Adsorbent:

- According to the first law of thermodynamics:

$$\frac{dU}{dt} = \dot{H} + \dot{Q}$$

$$\mathrm{u_{ad}}(\mathrm{T_{ad}}, \mathrm{w_{ad}})\frac{dm_{\mathrm{ad}}}{dt} + [m_{\mathrm{ad}}c_{\mathrm{ad}} + m_{\mathrm{sor}}\mathrm{c_{sor}}]\frac{d\mathrm{T_{ad}}}{dt}$$
$$= \dot{m}_{\mathrm{E}} h^{\mathrm{v}}(T_{\mathrm{E}}, p_{\mathrm{E}}) - \dot{Q}_{\mathrm{hx,A-sor}} - \dot{Q}_{\mathrm{sor-casing,A}}$$

$assumption\!: \mathrm{T_{ad}} = \mathrm{T_{sor}}$

for $adsorption\!: p_{\mathrm{E}} > p_{\mathrm{ad}}$

$\mathrm{u_{ad}} = f(\Delta h_{\mathrm{Ads}})$ … $from\ equilibrium\ data\ (derived\ from\ experiments\ and, e.g., Dubinin - Asthakhov\ correlation)$

$*_{\mathrm{ad}}\dots$ adsorbate (adsorbed phase)
$*_{\mathrm{sor}}\dots$ (ad-)sorbent
$*_{\mathrm{A}}\dots$ adsorber (reactor)
$*_{\mathrm{C}}\dots$ condenser
$*_{\mathrm{E}}\dots$ evaporator
$*_{\mathrm{hx}}\dots$ heat exchanger
$w\dots$ adsorbate loading [$\mathrm{kg_{ad}/kg_{sor}}$]
$u\dots$ specific internal energy [J/kg]
$T\dots$ temperature [K]
$p\dots$ pressure [Pa]
$c\dots$ specific heat capacity [J/(kg.K)]
$\Delta h_{\mathrm{Ads}}\dots$ specific enthalpy of adsorption [J/kg]
$\dot{Q}\dots$ heat flow rate [W]
$h^{\mathrm{v}}\dots$ specific enthalpy of the pure adsorptive (vapor) [J/kg]

Figure 2 Energy balance equation for the sorption material (adsorbent) during the adsorption process in the adsorber/reactor

For the development of the numerical models the modeling and programming language Modelica[1] and the development and simulation environment Dymola[2] were used. The applied modeling approach is referred to in the literature as the so-called "lumped parameter approach" (Cabeza 2020). That means that each component (e.g., the adsorber) is discretized as a "lumped object" (i.e., a single-node or multi-node model) and that for each node/cell the spatial variation of temperature, pressure, etc. is largely neglected and considered constant.

The numerical models of the storage system (sorption material, adsorber/reactor, evaporator/condenser) were developed, adapted and parameterized according to the laboratory test rig of the closed sorption system (see next chapter). The numerical models are based on existing models from the Modelica libraries "Modelica Standard Library" (version 3.2.3)[3] and “SorpLib” (version 2.0)[4], which were adapted accordingly. The implementation of the sorption equilibrium model of the working pair water and zeolite 13XBF, using the well-known Dubinin-Astakhov correlation, was realized with the help of a library for sorption properties named "SorpPopLib"[5] and by means of the corresponding Python and Modelica interfaces. Figure 3 shows the laboratory test rig and the sorption storage system in the development and simulation environment Dymola.

3.4 System simulation

The system simulation is based on the specific procedural features of the open and closed sorption systems, which differ in their boundary conditions. The principle of operation of typical reactor elements is shown in Figure 4. These elements can be enlarged and combined into a more complex system to represent the storage system. Specific operating situations such as partial loading, diffusion, external losses, and internal leveling processes within the system and material changes (degradation) must be represented separately from the typical cells.

---

[1] https://modelica.org/modelicalanguage.html (accessed on 25.02.2023)

[2] https://www.claytex.com/wp-content/uploads/2018/06/Dymola-Referential.pdf (accessed on 25.02.2023)

[3] https://github.com/modelica/ModelicaStandardLibrary (accessed on 25.02.2023)

[4] https://git.rwth-aachen.de/ltt/SorpLib/-/tree/SorpLib_v2 (accessed on 25.02.2023)

[5] https://github.com/zhiyaoYang/sorpproplib_JSON (accessed on 25.02.2023)

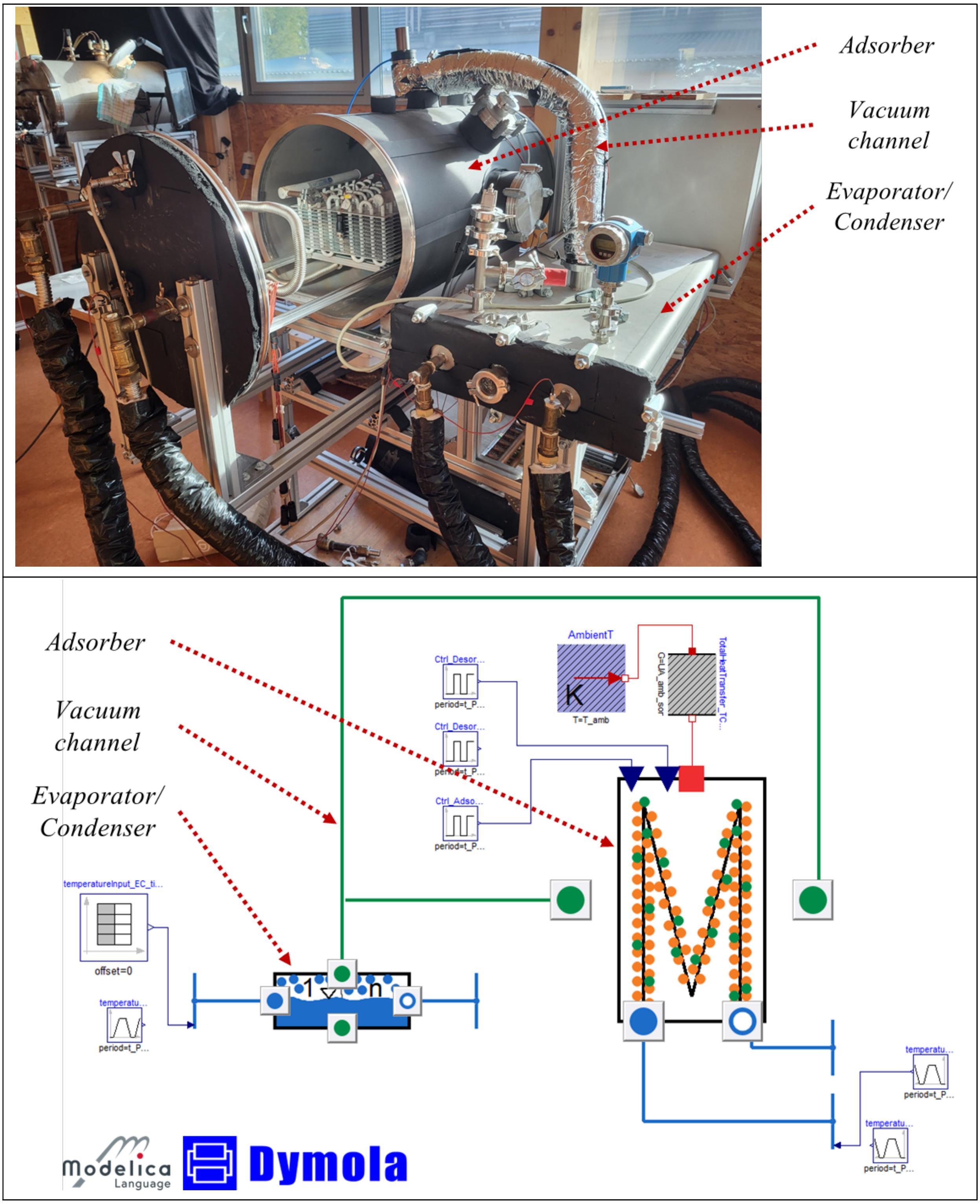

Figure 3: Laboratory test rig (top) and sorption storage system in the development and simulation environment Dymola (bottom)

The SOC determination on the three levels, material properties, local SOC, and system SOC is intended to largely rule out errors:

- The material calibration procedure determines the relationship between the physical sensor signal and material properties
- The filter algorithm and the adsorption model verify the material property changes based on the process parameters and determine the (local) material loading,
- The storage simulation model considers the process technology and operational management of the entire system (the sum of all cells and boundary conditions)

Using this step-by-step approach and with the help of an experimental setup and measured data for training and demonstrating the virtual sensor operation, a sophisticated approach to SOC determination for thermochemical storage is developed and a reliable metric for process control is developed.

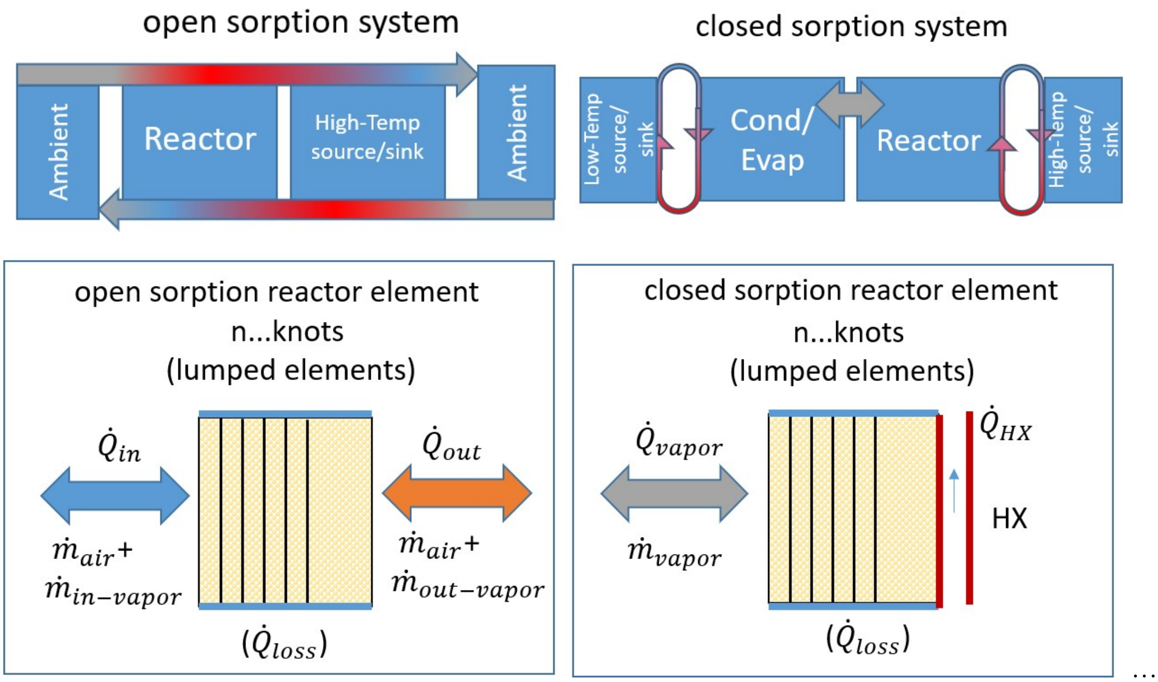

Figure 4: Operating principle of the closed and open sorption TES (above) and the boundary conditions of two typical reactor elements

4 Experimental Results

4.1 Open Sorption Reactor

In an open moving bed reactor, a capacitive sensor is used between which electrodes the material is allowed to move freely (Fig. 5). Depending on the moisture content of the material, the electrical permittivity changes and with it the effective capacitance value of the capacitor.

To record the signal, the capacitor is integrated into a parallel resonant circuit and the resonant frequency of the resonant circuit is reacting on the moisture content of the material. The resonant frequency is therefore used as a relatively sensitive but stable indicator of the material moisture. The resonant frequency of the oscillating circuit is around 196 kHz, the capacitance of the unfilled capacitor 8.8 pF. A turntable with a diameter of 100 cm and a material volume of 15 litres simulates the moving bed of a storage system. The rotating speed of the disk is about 5 revolutions per minute.

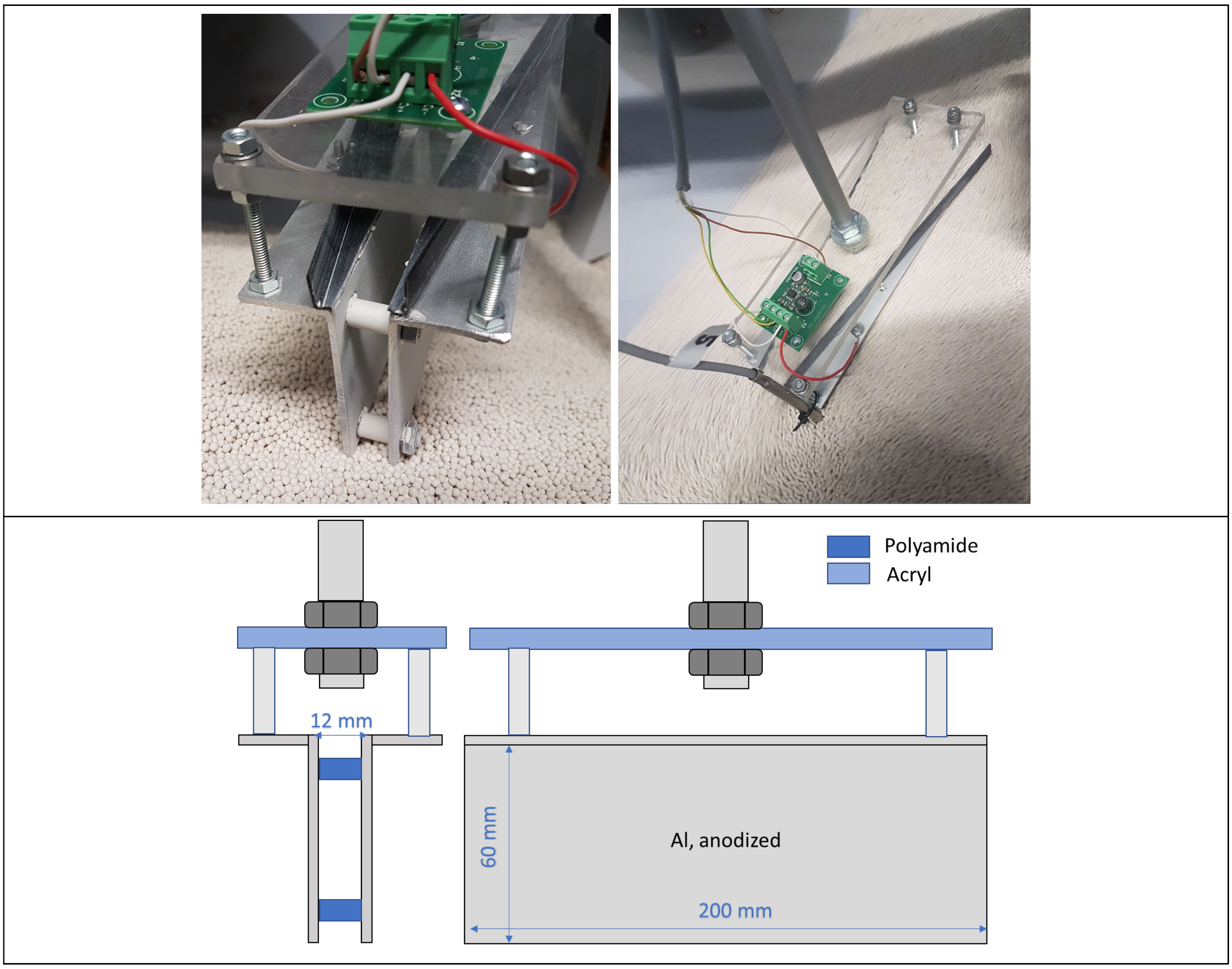

Figure 5 Parallel plate capacitor placed in a moving bed of zeolite granules of 1.5-2.5mm

The dehydrated zeolite (12h @ 250°C) is filled into the turntable and ventilated with moist air from an ultrasonic fogger. Samples are taken at periodic intervals and the material moisture is measured using the reference measurement (2 hours in a drying furnace @ 350°C). The measurement ends when no further moisture increase is recognized in the zeolite bed[6]. The measurement result for two types of zeolite in four different varieties is shown in the figures below.

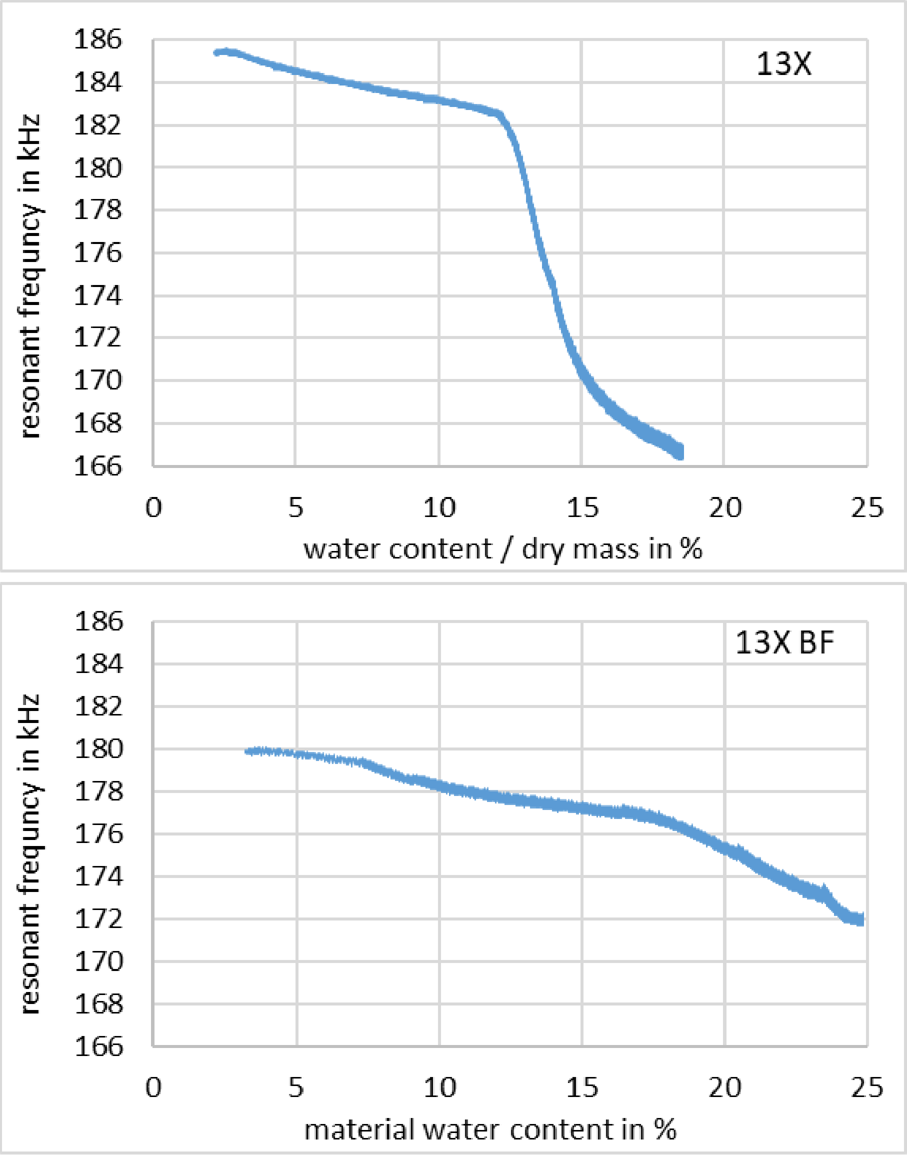

Figure 6: Measured resonant frequency during the adsorption experiment at low temperature (25-40°C) in zeolite 13X (top) and 13X binder free (right), both 1.5-2.5 mm granules (bottom).

---

[6] Humidity saturation according to the producer datasheet may be 5-10% higher than reached in this experiment

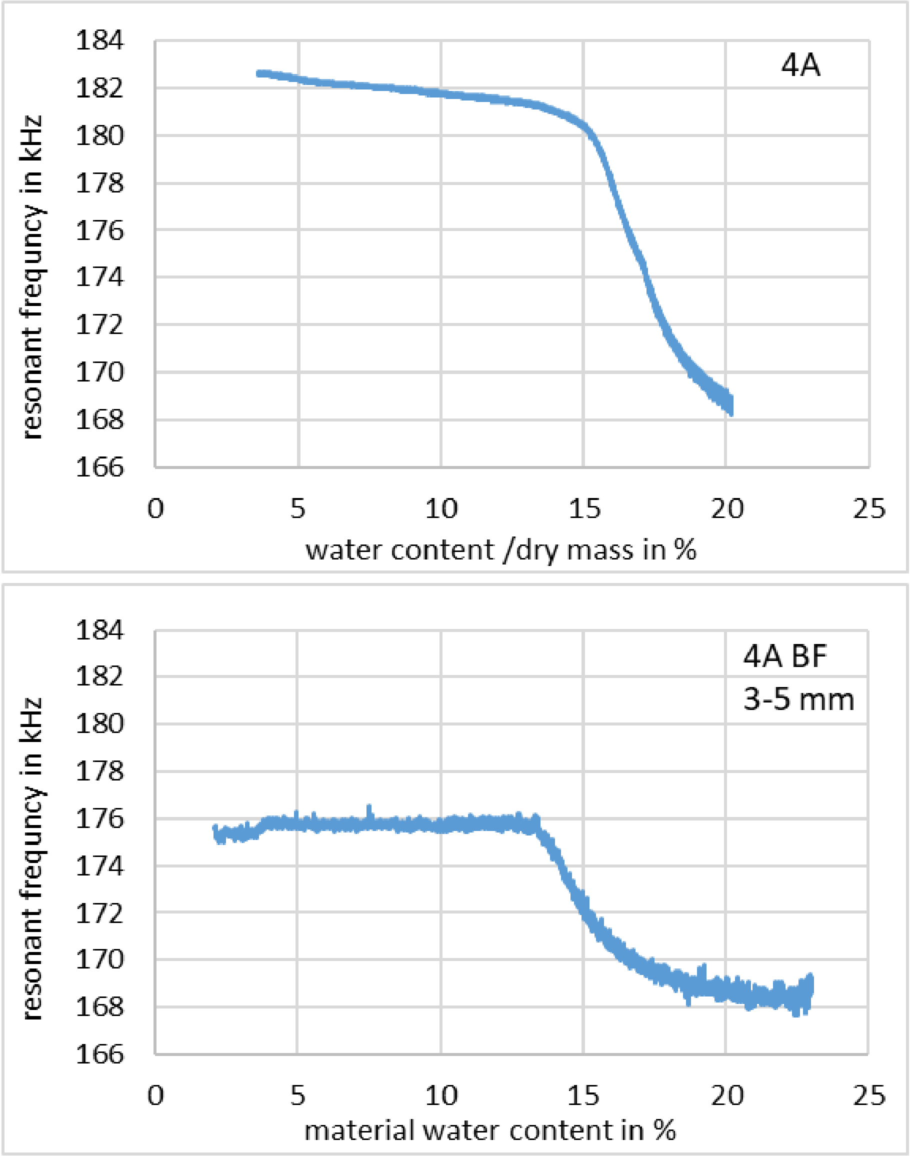

Figure 7: Measured resonant frequency during the adsorption experiment at low temperature (25-40°C) in zeolite 4A 1.5-2.5 mm granules (top) and 4A binder free, 3-5 mm granules (below).

The results of the experiments show a clear influence of the material humidity on the resonant frequency. In general, the higher the humidity the lower the resonant frequency, but influence is non-linear: rate of frequency drop at the beginning of the experiment (dry material) is lower, for more humid material frequency drop is higher. For 4A-BF, no frequency change until approx. 13 wt.% of water was detected.

The temperature also plays a certain role, in general, higher temperatures tend to lower the resonant frequency. For adsorption reactions in the range of 30-50°C, the temperature plays no important role for zeolite 13X since the humidity influence is dominant. For other zeolites such as 4A-BF further calibration measurements should lead to a kind of temperature correction term for the resonant frequency. For high temperature desorption application (150-

250°C) of the suggested measurement principle, separate calibration measurement would be necessary.

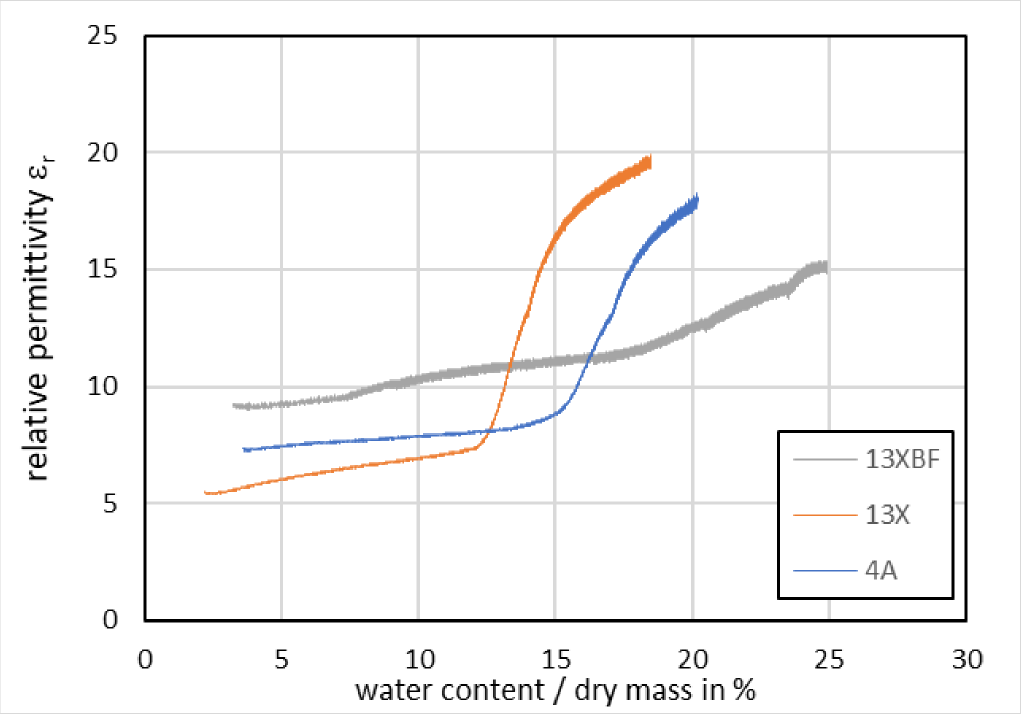

Figure 8 Calculated relative permittivity of different zeolites

As mentioned earlier the resonant frequency relies on the active capacity in the electronic oscillator, while the capacity value itself consist of the addition of several parts: the electronic capacity inside the electronic circuit (C_p), the capacity of the sensor cable (C_C), and the sensor itself including the material (C_s). The built-in components of the oscillator are C_p=470 pF and L=1.4 mH, the oscillator-print itself (without external components) exhibit an resonance frequency of 196.11 kHz.

$$f_r = \frac{1}{2\pi\sqrt{LC}} \quad \dots .\, resonant\ frequnecy$$

$$C = C_p + C_c + C_s \dots .\, capacity$$

$$C_s = \varepsilon \frac{A}{d}, \quad \varepsilon = \varepsilon_r \varepsilon_0, \quad \varepsilon_0 = 8{,}845\ 10^{-12} As/Vm$$

$$\varepsilon_r = \frac{1}{\varepsilon_0}\frac{d}{A}\left(\frac{1}{L}\left(\frac{1}{2\pi f_r}\right)^2 - C_p - C_c\right)$$

A certain drop of the resonant frequency indicates an increase of the sensor capacity C_s, according to above equations due to an increase of relative permittivity ε_r according to eq.3. After connecting sensor and cable to the oscillator resonance frequency decreases by 3.3 kHz, which corresponds to an additional capacity C_c+C_s= 16.5 pF while C_s= 8,9 pF

(according to eq.3). By measuring the further frequency decrease after inserting into the zeolite bed the permittivity of the material while humidified can be calculated.
Calculating the relative permittivity out of the recorded frequencies leads to the results shown in Figure 8. The permittivity of the dry zeolite is in the range of ε_r =5….10, while in the hydrated material ε_r rises to 15…20. For comparison, dielectric properties of various minerals can be found in the literature. The values for sand or clay with a material moisture content between 0…..20% are comparable, with measured values of ε_r in the range of 5 to 20.
In literature the development of the dielectric constant is explained with the help of a multiphase model. In porous minerals and soils, water fraction below the point WP"[7] (Fig. 9) are addressed as "bound water", above the porosity point P as "free water" and between as "mixed state", producing a multi-phase signal (Park, C.-H., et.al., 2017). In adsorption process engineering, the multiphase model refers to the formation of layers of adsorbate in the pores of the adsorbent: the first layer is bound more strongly than the second and subsequent ones, which form capillary condensation.

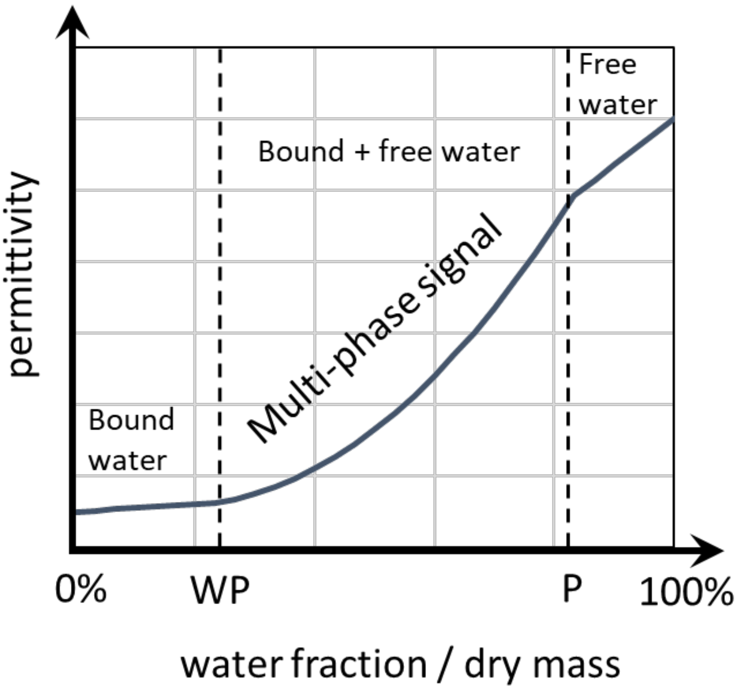

Figure 9: Multiphase model of dielectric constant (permittivity) of humid minerals, redrawn from (Park, C.-H., et.al., 2017)

---

[7] wilting point WP, refers to a certain water fraction, below which water is bound by adsorption in clay and soil and plants are not able to benefit from it.

4.2 Closed Sorption Reactor

For the application in a closed sorption vessel, there are several challenges for the sensor technology, such as vacuum resistance, resistance to high temperatures (up to 200°C) during desorption, the influence of the measurement signal by the fixed-bed heat exchanger and by the locally different reaction states in the storage tank.

The test stand (Figure 10) is equipped with numerous temperature sensors, a scale for estimating the state of charge and pressure sensors on the adsorber and evaporator. Numerous charging and discharging tests were carried out with different boundary conditions. We had to disregard the results of the scales due to their strong temperature dependency. The test bench was already used in the "Tes4seT" project, for example, and was adapted and optimized in a few points to the changed requirements. For example, the electrical connections of the measuring probe were routed through the outer shell of the adsorber.

The heat exchanger filled with zeolites, shown in Figure 11, is located in the adsorber. In the middle of this heat exchanger is the measuring probe that is used to determine the moisture content of the zeolite. Temperature-controlled liquid (heat transfer oil) flows through the heat exchanger from outside the adsorber. With the help of temperature control, among other things, the adsorption and desorption of the zeolite material can be started or controlled.

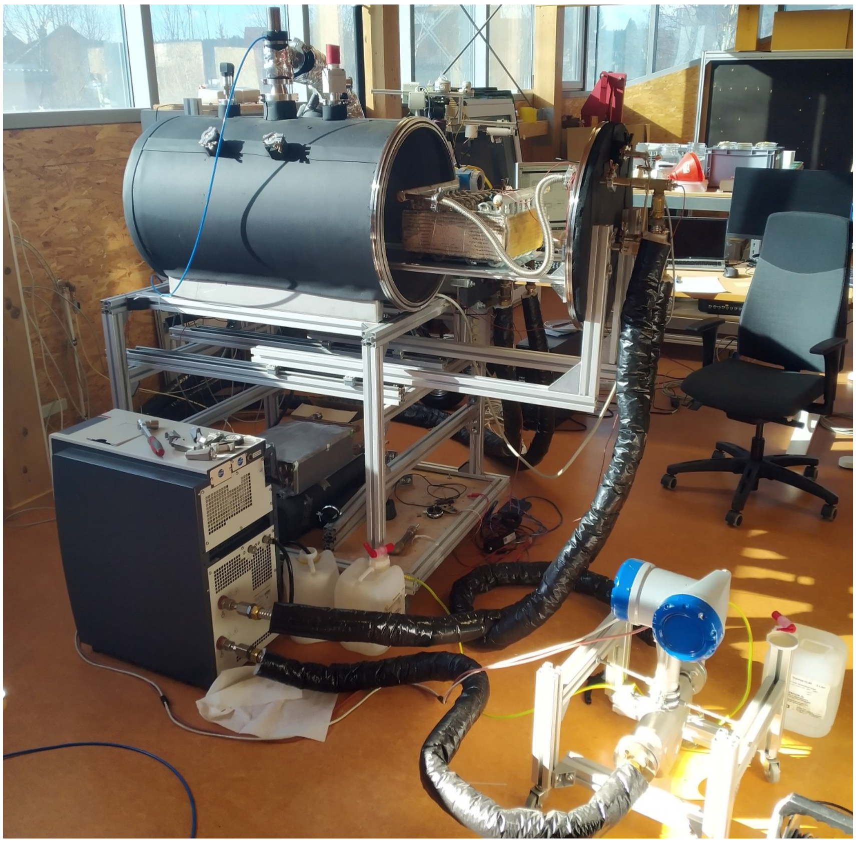

Figure 10: Setup- Closed Sorption

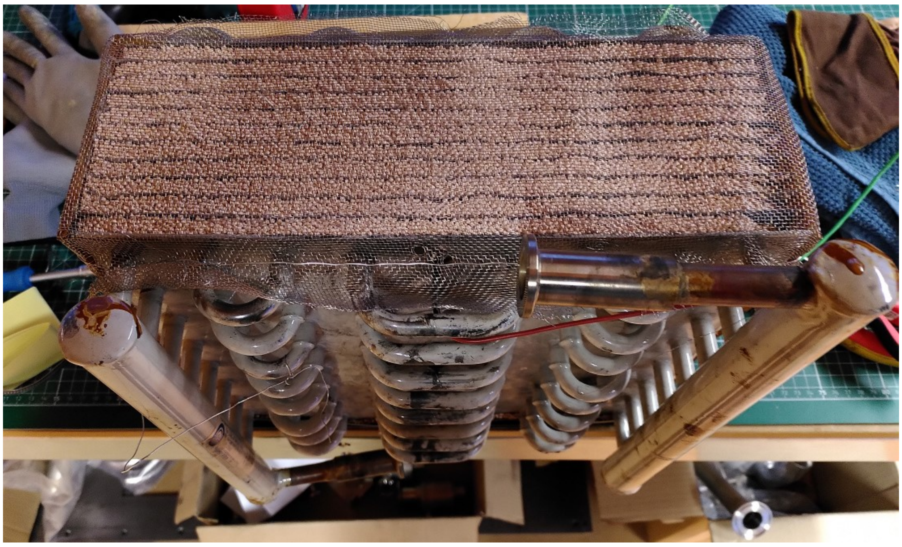

Figure 11: Details of the Heat Exchanger

As shown in Figure 12, a sector cylinder capacitor (SCC) was developed, which contains in the inside the same sorption material as the rest of the storage tank. The water uptake of the internal sorption material inside the enclosure influences the capacitor and the measurement, therefore. Due to the large dimension of closed sorption vessels several regions are covered by linked sectors of the cylindrical capacitor.**Fehler! Verweisquelle konnte nicht gefunden werden.**Figure 13 shows a picture of several coupled sectors, so that several areas in the fixed-bed storage tank can be measured simultaneously with one sensor installation.

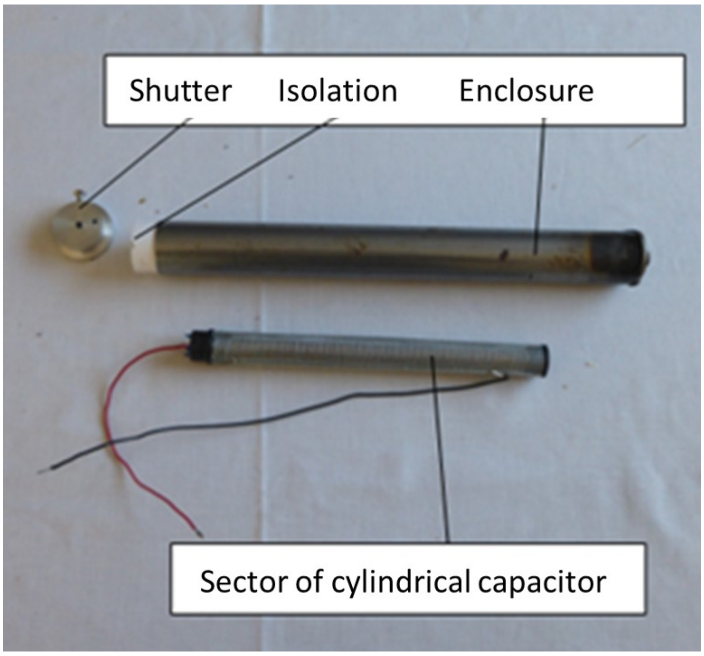

Figure 12: Setup of the cylinder capacitor

Figure 13: Coupling of several sector cylinder capacitor

Figure 14 shows the characteristic frequency curves of the zeolite 13X BF as a function of the temperature and the degree of humidity in a fixed bed reactor. They act as the basis for programming a microprocessor when the measured frequencies and temperatures are interpreted as the degree of humidity in the measured sector.

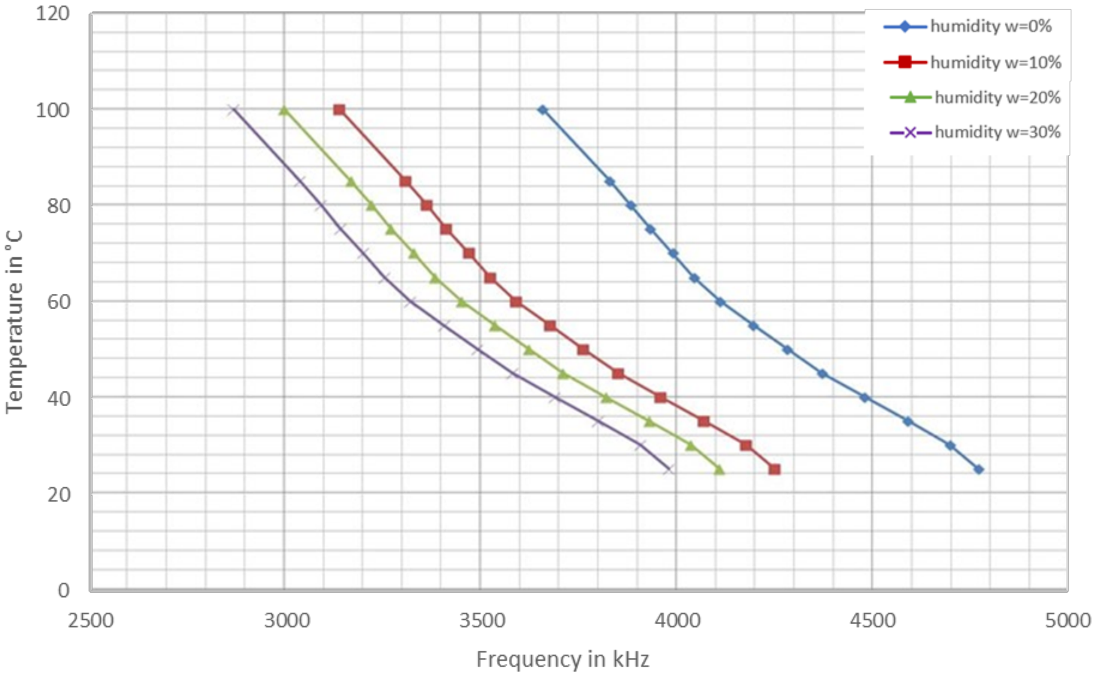

Figure 14: Characteristic frequencies of zeolite 13X BF as a function of the temperature and the degree of humidity

The preliminary tests have shown that both the moisture, which accumulates in the form of water films in the molecular area of the zeolite material, and the temperature of the zeolite material have a major influence on the dielectric constant. If one now wants to determine the degree of moisture at one point of the bed at different material temperatures, the temperature of the zeolite bed must also be measured at the same point. In the first step, a family of characteristics was determined for the zeolite 13XBF material used, which shows a direct relationship between the dielectric constant (ordinate) and the temperature (abscissa), with the humidity level as a parameter (see Figure 15). Several series of measurements were made for this family of characteristics.

When the measurements were carried out, there were deviations in the range of 5% due to the uneven density of 13XBF in the SCC. Repeated filling of the SCC using the same procedure showed that different 13XBF densities were achieved each time. However, different filling densities have a direct influence on the displayed resonant frequency, which is a measure of the dielectric constant.

It should also be mentioned that the 13XBF samples came from two sample preparations that took place at different times, but were always stored in airtight containers. The samples 10%, 20% and 30% were filled and measured several times in SCC's. Especially with high humidity and high temperatures, the oscillator performance had to be increased through changes in the electronics, and the corresponding measurement had to be repeated.

In order to investigate this temperature dependency, several test series were carried out. The result can be seen in Figure 15.

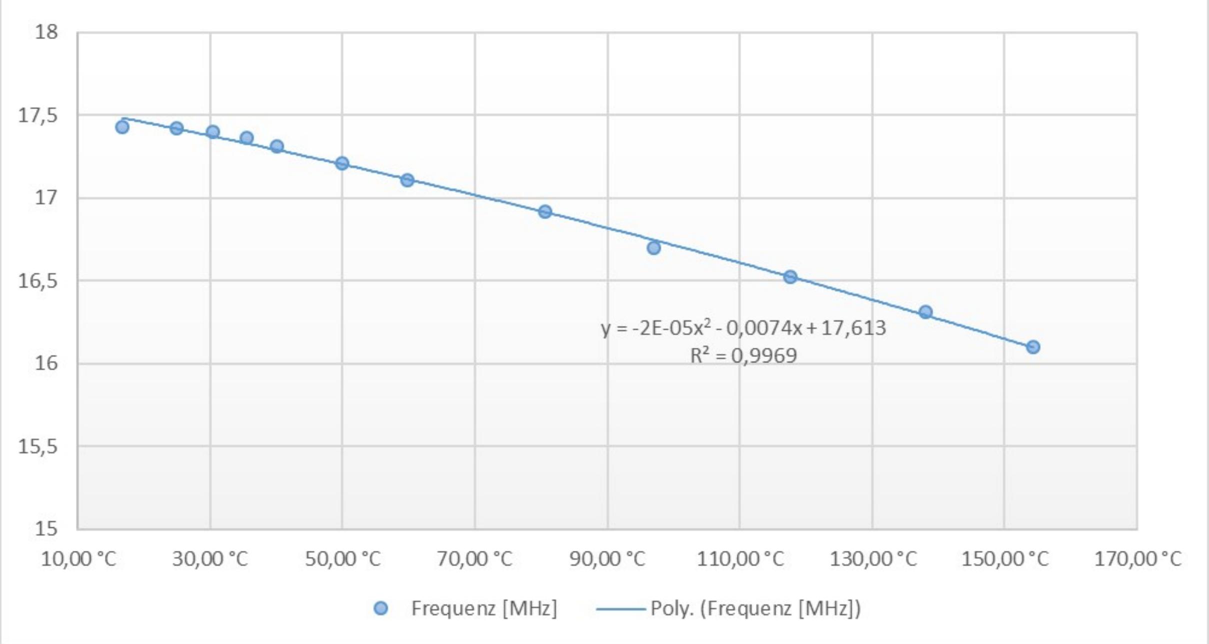

Figure 15: Temperature dependency of the dielectric constant at a material water content of 16%

With the help of this curve and the formula of the trend line, the temperature dependence can be calculated from the results of the previous measurements at a load of 16%.

This temperature dependency would now have to be measured for several loading states in order to be able to cover the entire loading range.

5 Filter Development

A Kalman Filter is a virtual dynamical system (a computer algorithm) which is generating an online estimate $\hat{x}$ of the current state x of a real dynamical system based on the history of input (u) and output (y) measurement data from the real system and a mathematical model of the system (Grewal and Andrews 2001). There are numerous applications of Kalman filters as real-time estimators, for example SOC and state of health estimation in battery cells, estimation of position and orientation of moving objects such as quadcopters for example, based on easily available accelerometer measurements. In general, it enables to estimate an internal quantity of a process which is otherwise not accessible through direct measurement, hence the alias “virtual sensor”. Since the filter works with real-time measurement data, its results are affected by the corresponding measurement noise. However, under certain statistical assumptions (Simon 2006) it can be guaranteed that the Kalman Filter is a mathematically optimal estimator for linear systems in the sense that the covariance of the state estimation error is minimized.

5.1 Adsorption Model Adaption and Kalman Filter Development: Open System

The concept of the Kalman Filter is applied to the problem of determining the current state of charge of a sorption storage system. Here, we are considering a fixed-bed sorption storage using zeolite as sorption material as it was presented and mathematically modelled in Daborer-Prado, N., et.al. (2020). This model forms the basis for the model development required for the Kalman Filter. We are considering the 1-node model (the entire longitudinal direction of the storage is considered as one element with one lumped parameter for the water load) which uses as internal states to describe the dynamics

$$x = [x_s \quad x_G \quad T_s \quad T_{brd}]^T$$

where x_s is the water load of the sorptive material, x_G is the water load of the gas flowing through the storage, T_s is the temperature of the sorptive material, and T_{brd} is the temperature on the storage exterior. The model inputs are

$$u = [m_G^{IN} \quad x_G^{IN} \quad T_G^{IN}]^T$$

where m_G^{IN} is the mass flow of the gas through the storage, x_G^{IN} is the absolute humidity of the gas flow with respect to dry air, and T_G^{IN} is the temperature of the inflow gas. For details of the model development, we refer to the paper Daborer-Prado, N., et.al. (2020). The mathematical model to be used in the design phase of the Kalman Filter differs from the described simulation model. One central difference is the way how the water load x_G is treated: in the simulation model a spatial differential equation describes its behavior with

respect to the longitudinal direction, while temporal differential equations describe the outcome of the outflow water load x_G^{OUT} at the point where gas leaves the storage, depending on the other state variables x. A standard Kalman Filter requires a system of ordinary differential equations, therefore model adaptations were made in the following way:
A data-driven state space model of second order was developed which approximatively provides the quantity x_G^{OUT} as output and uses the quantities (x_s, T_S) as input. To estimate this model, data sequences at various stationary choices of the inputs u were generated using the simulation model. The estimated model obtained fit-values (a measure of the coincidence of model output and data sequences) of more than 90% on all datasets. This model contains two new state variables x_1 and x_2. The overall mathematical model for the Kalman Filter combines those two states with the ones from the simulation model described above to the augmented state vector

$$x_{KF} = [x_s \quad x_1 \quad x_2 \quad T_S \quad T_{brd}]^T$$

Further assumptions were made in the development process of the Kalman Filter:

- The input x_G^{IN} was assumed to be constant throughout an experiment
- The input T_G^{IN} was assumed to be constant throughout an experiment
- The states T_S and T_{brd} are assumed to be accessible through measurement on the device

Altogether, the mathematical model can be described in the general form of a continuous time nonlinear state-space model with the state x_{KF} and the input m_G^{IN}:

$$\dot{x}_{KF} = f(x_{KF}, m_G^{IN})$$

As a next step, the model needs to be transferred into discrete-time. For this purpose, a simple Euler approximation with a sample time ΔT is utilized and given in the general formulation:

$$x_{k+1} = x_k + \Delta T\, f(x_k, u_k)$$

Note that this model is non-linear since the dynamics of the original simulation model are also nonlinear. Therefore, a standard linear Kalman Filter is not applicable and the extension of an extended Kalman Filter (EKF), see e.g. (Grewal and Andrews 2001) capable of dealing with nonlinearities could be used instead. A natural approach would also be to linearize the model around one stationary operating point and assume “small” deviations from this point during operation. There is, however, no stationary operating point in the considered application since the load x_s will continue to rise (in adsorption mode) even if all the input quantities are fixed to constant values inside the operating conditions. Therefore, an EKF was developed and implemented in the MATLAB® /Simulink^{TM} environment using the built-in EKF functionality. The general overview of the system can be seen in Figure 16.

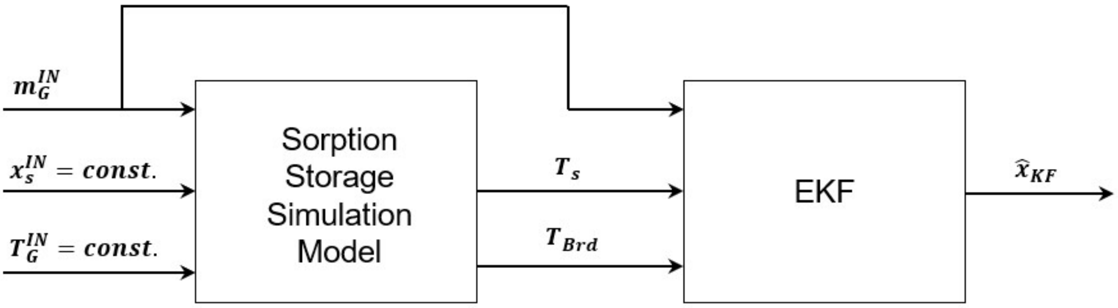

Figure 16: Signal flow and connections of the EKF with the simulation model

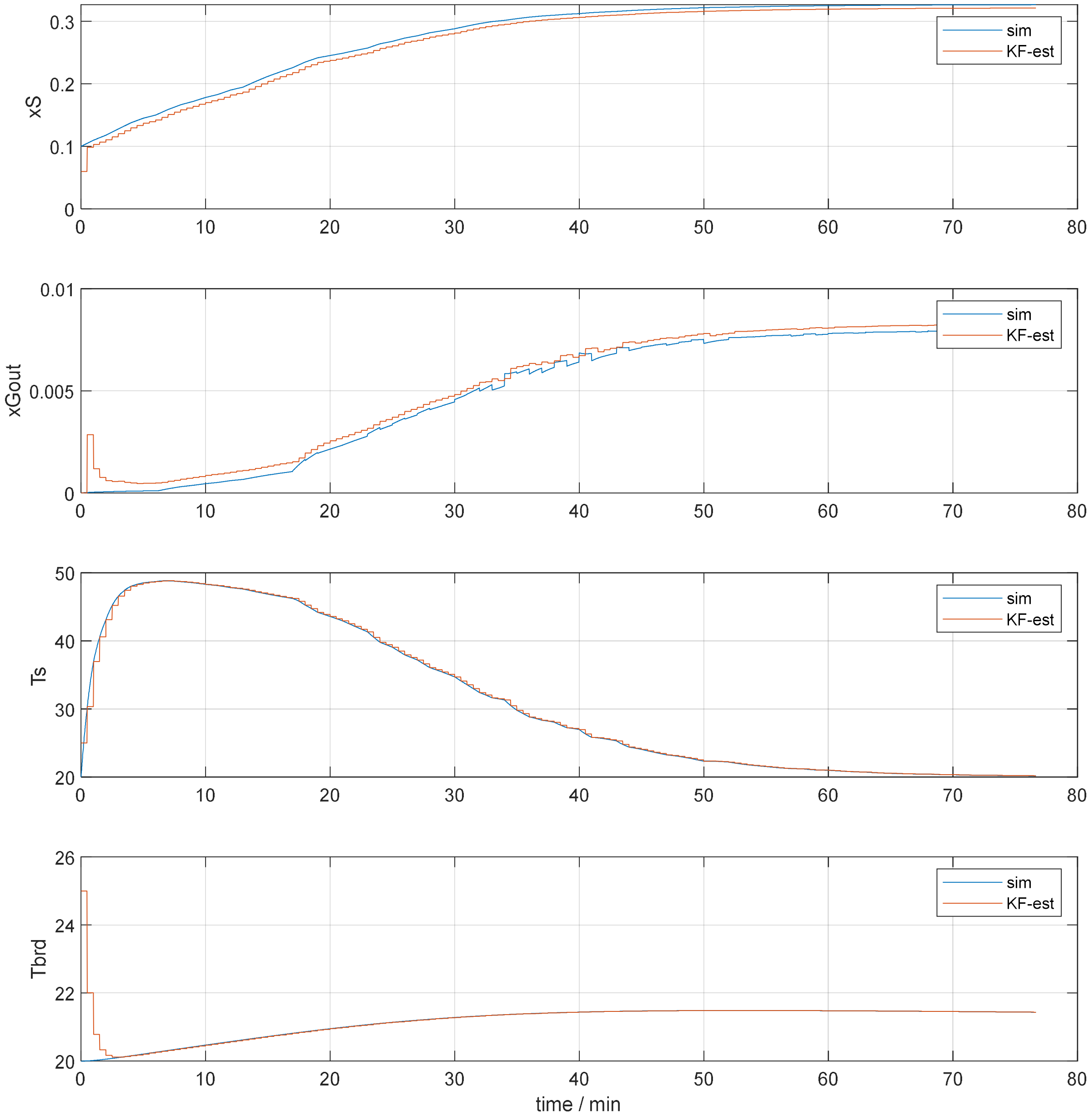

Figure 17: Comparison of the EKF-estimated states with the simulation model for the open sorption storage system

To demonstrate the quality of the state estimation, a simulation where the input was chosen to $m_G^{IN} = 300$ kg/h and the sorption material had an initial humidity of $x_S(t = 0) = 0.1$ was performed. The results are graphically shown in Figure 17: Comparison of the EKF-estimated states with the simulation modelFigure 17 where the blue lines represent the quantities derived from the simulation model and the red lines are the state estimates from the EKF. Since the initialization of the EKF does not match precisely the initial conditions of the simulation model (which is a realistic assumption), there are minor deviations between the two lines in the beginning of the experiment. This is an expected behaviour of virtually any Kalman Filter application unless initial states are perfectly known. As the experiment continues, the lines begin to coincide, especially the two temperatures shown in the bottom two panels. This is because those temperatures are directly measured and the tuning of the EKF was done in such a way that the errors introduced in those measurements are assumed to be small in comparison to the errors introduced in the modelling of the states x_S and x_G. In other words, the measurement covariance was chosen much smaller than the covariance of the additive process noise affecting the model states. With respect to the actual variable of interest, the water load x_S, shown in the top panel, the EKF can reproduce its trajectory in a sufficient way and only introduces a minor offset.

5.2 Adsorption Model Adaption and Kalman Filter Development: Closed System

The closed sorption storage system model described in chapter 2.2 formed the basis for the model development required for the Kalman Filter. For the real-time application in the Kalman filter the mathematical model of the detailed simulation model was simplified and an assignment into state, measured and input variables as well as parameters was made. Figure 18 shows the mathematical description of the detailed simulation model, the simplifications made and the assignment in parameters, input, state and measured variables for the adsorption process for the application in the Kalman filter.

Based on this simplified model description, the corresponding dynamic state equations were derived and discretized using an Euler approximation. The resulting difference equations for the three states are given by equation (1), along with the discrete version of the algebraic equations which are given by equation (2). Note that the state equations are nonlinear differential equations, hence, an extended Kalman Filter was required in this case since a linear approximation of the equations resulted in unacceptable loss of model performance. The developed virtual sensor was tested in a simulation environment, where it was connected to pre-recorded data from a Dymola simulation of the closed sorption storage system. The results are graphically displayed in Figure 20: Comparison of the EKF estimated states with the simulation model for the closed sorption storage system. a good agreement between the estimated water saturation (w_{ad}) and the simulated signal.

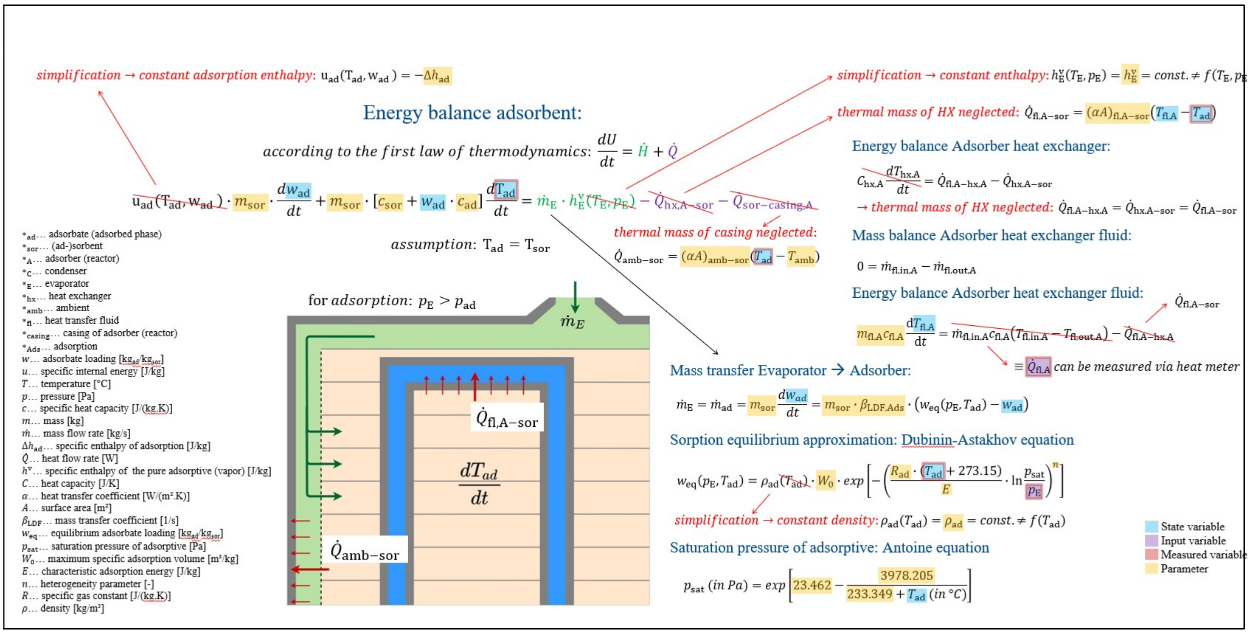

simplification → constant adsorption enthalpy: $u_{ad}(T_{ad}, w_{ad}) = -\Delta h_{ad}$

Energy balance adsorbent:

according to the first law of thermodynamics: $\frac{dU}{dt} = \dot{H} + \dot{Q}$

$$\cancel{u_{ad}(T_{ad}, w_{ad})} \cdot m_{sor} \cdot \frac{dw_{ad}}{dt} + m_{sor} \cdot [c_{sor} + w_{ad} \cdot c_{ad}] \frac{dT_{ad}}{dt} = \dot{m}_E \cdot h_E^v\cancel{(T_E, p_E)} - \cancel{\dot{Q}_{hx,A-sor}} - \cancel{\dot{Q}_{sor-casing,A}}$$

assumption: $T_{ad} = T_{sor}$

thermal mass of casing neglected: $\dot{Q}_{amb-sor} = (\alpha A)_{amb-sor}(T_{ad} - T_{amb})$

for *adsorption:* $p_E > p_{ad}$

simplification → constant enthalpy: $h_E^v(T_E, p_E) = h_E^v = const. \neq f(T_E, p_E)$

thermal mass of HX neglected: $\dot{Q}_{fl,A-sor} = (\alpha A)_{fl,A-sor}(T_{fl,A} - T_{ad})$

Energy balance Adsorber heat exchanger:

$$\cancel{C_{hx,A} \frac{dT_{hx,A}}{dt}} = \dot{Q}_{fl,A-hx,A} - \dot{Q}_{hx,A-sor}$$

→ thermal mass of HX neglected: $\dot{Q}_{fl,A-hx,A} = \dot{Q}_{hx,A-sor} = \dot{Q}_{fl,A-sor}$

Mass balance Adsorber heat exchanger fluid:

$$0 = \dot{m}_{fl,in,A} - \dot{m}_{fl,out,A}$$

Energy balance Adsorber heat exchanger fluid:

$$m_{fl,A} c_{fl,A} \frac{dT_{fl,A}}{dt} = \cancel{\dot{m}_{fl,in,A} c_{fl,A}(T_{fl,in,A} - T_{fl,out,A})} - \cancel{\dot{Q}_{fl,A-hx,A}}$$

$\dot{Q}_{fl,A-sor}$

$\equiv \dot{Q}_{fl,A}$ *can be measured via heat meter*

Mass transfer Evaporator → Adsorber:

$$\dot{m}_E = \dot{m}_{ad} = m_{sor} \frac{dw_{ad}}{dt} = m_{sor} \cdot \beta_{LDF,Ads} \cdot (w_{eq}(p_E, T_{ad}) - w_{ad})$$

Sorption equilibrium approximation: Dubinin-Astakhov equation

$$w_{eq}(p_E, T_{ad}) = \rho_{ad}\cancel{(T_{ad})} \cdot W_0 \cdot exp\left[-\left(\frac{R_{ad} \cdot (T_{ad} + 273.15)}{E} \cdot \ln \frac{p_{sat}}{p_E}\right)^n\right]$$

simplification → constant density: $\rho_{ad}(T_{ad}) = \rho_{ad} = const. \neq f(T_{ad})$

Saturation pressure of adsorptive: Antoine equation

$$p_{sat}\,(in\ Pa) = exp\left[23.462 - \frac{3978.205}{233.349 + T_{ad}\,(in\ °C)}\right]$$

🟦 State variable
🟪 Input variable
🟥 Measured variable
🟨 Parameter

$*_{ad}$… adsorbate (adsorbed phase)
$*_{sor}$… (ad-)sorbent
$*_{A}$… adsorber (reactor)
$*_{C}$… condenser
$*_{E}$… evaporator
$*_{hx}$… heat exchanger
$*_{amb}$… ambient
$*_{fl}$… heat transfer fluid
$*_{casing}$… casing of adsorber (reactor)
$*_{Ads}$… adsorption
w… adsorbate loading [kg_{ad}/kg_{sor}]
u… specific internal energy [J/kg]
T… temperature [°C]
p… pressure [Pa]
c… specific heat capacity [J/(kg.K)]
m… mass [kg]
$\dot{m}$… mass flow rate [kg/s]
Δh_{ad}… specific enthalpy of adsorption [J/kg]
$\dot{Q}$… heat flow rate [W]
h^v… specific enthalpy of the pure adsorptive (vapor) [J/kg]
C… heat capacity [J/K]
α… heat transfer coefficient [W/(m².K)]
A… surface area [m²]
β_{LDF}… mass transfer coefficient [1/s]
w_{eq}… equilibrium adsorbate loading [kg_{ad}/kg_{sor}]
p_{sat}… saturation pressure of adsorptive [Pa]
W_0… maximum specific adsorption volume [m³/kg]
E… characteristic adsorption energy [J/kg]
n… heterogeneity parameter [-]
R… specific gas constant [J/(kg.K)]
ρ… density [kg/m³]

Figure 18 Mathematical description of the detailed simulation model, simplifications and the assignment into parameters, input, state and measured variables for the adsorption process for application in the Kalman filter

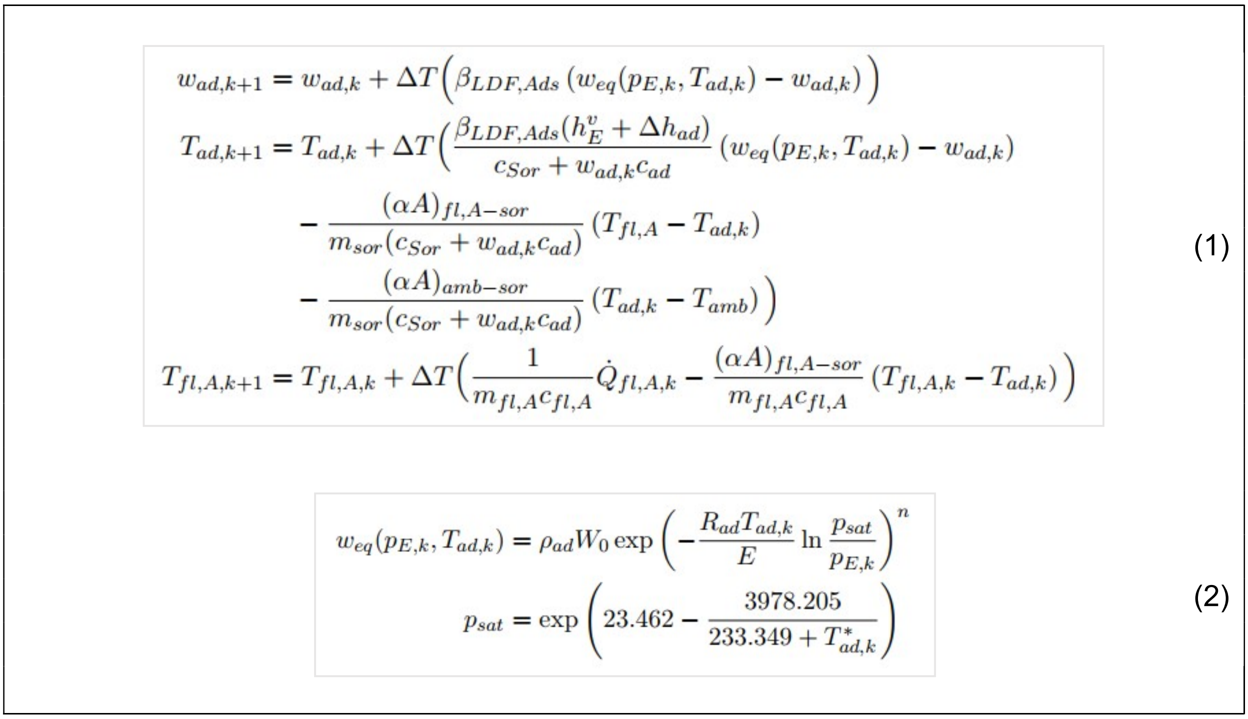

$$
\begin{aligned}
w_{ad,k+1} &= w_{ad,k} + \Delta T\left(\beta_{LDF,Ads}\left(w_{eq}(p_{E,k}, T_{ad,k}) - w_{ad,k}\right)\right) \\
T_{ad,k+1} &= T_{ad,k} + \Delta T\left(\frac{\beta_{LDF,Ads}(h_E^v + \Delta h_{ad})}{c_{Sor} + w_{ad,k}c_{ad}}\left(w_{eq}(p_{E,k}, T_{ad,k}) - w_{ad,k}\right)\right. \\
&\quad - \frac{(\alpha A)_{fl,A-sor}}{m_{sor}(c_{Sor} + w_{ad,k}c_{ad})}\left(T_{fl,A} - T_{ad,k}\right) \\
&\quad \left. - \frac{(\alpha A)_{amb-sor}}{m_{sor}(c_{Sor} + w_{ad,k}c_{ad})}\left(T_{ad,k} - T_{amb}\right)\right) \\
T_{fl,A,k+1} &= T_{fl,A,k} + \Delta T\left(\frac{1}{m_{fl,A}c_{fl,A}}\dot{Q}_{fl,A,k} - \frac{(\alpha A)_{fl,A-sor}}{m_{fl,A}c_{fl,A}}\left(T_{fl,A,k} - T_{ad,k}\right)\right)
\end{aligned}
\tag{1}
$$

$$
\begin{aligned}
w_{eq}(p_{E,k}, T_{ad,k}) &= \rho_{ad} W_0 \exp\left(-\frac{R_{ad}T_{ad,k}}{E}\ln\frac{p_{sat}}{p_{E,k}}\right)^n \\
p_{sat} &= \exp\left(23.462 - \frac{3978.205}{233.349 + T_{ad,k}^*}\right)
\end{aligned}
\tag{2}
$$

Figure 19: Simplified model

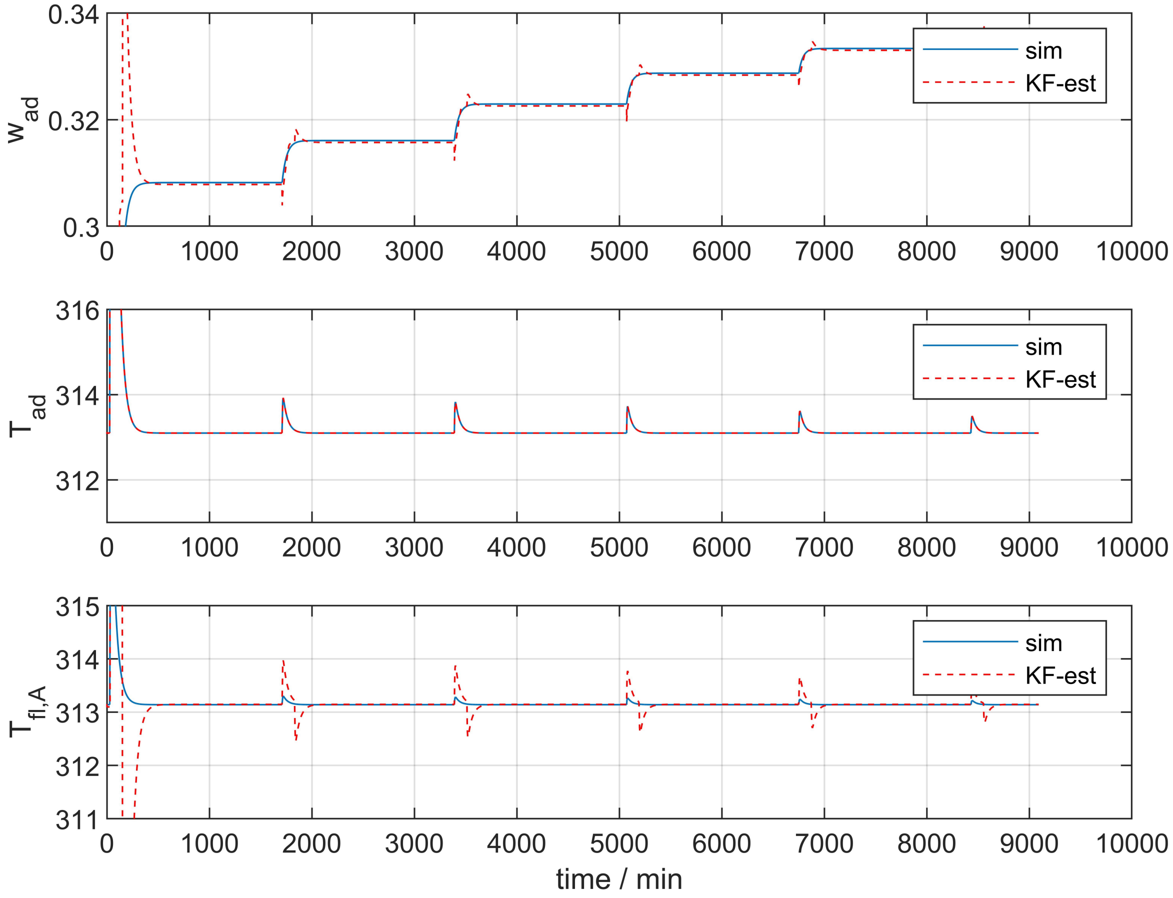

Figure 20: Comparison of the EKF estimated states with the simulation model for the closed sorption storage system.

6 Summary

In order to develop a new State-of-Charge (SOC) sensor, the concept of a virtual sensor concept was applied, combining physical measurements, adsorption model, and system simulation.

- Calibration data is used to exhibit the material relative permittivity dependence to the material humidity.
- In the 200 kHz frequency range, material water content is the dominant factor that influences the relative permittivity of 13X-BF zeolite in an open ad-sorption reactor, other materials like zeolite 4A show little changes likewise.
- In the 2 MHz frequency range, a pronounced influence of both, temperature and humidity was measured for closed adsorption.
- The Kalman-filter is suitable to repress sensor failures by estimating the material characteristics based on a modified adsorption model. The model allows the fast in-line prediction of the future material humidity load based on the current state, sensor signals and the modified adsorption model.

- A system simulation is suitable to integrate the virtual sensor into a reliable SOC determination of the entire storage system.

References

Cabeza, Luisa F. *Advances in Thermal Energy Storage Systems: Methods and Applications*. Second Edition. Woodhead Publishing Series in Energy. Woodhead Publishing, 2020.

Daborer-Prado, N., Kirchsteiger, H., Zettl, B., Asenbeck, S., Kerskes, H., 2020. Mathematical modeling of rotating sorption heat storages. Proceedings of the ISES Solar World Congress 2019 and IEA SHC International Conference on Solar Heating and Cooling for Buildings and Industry 2019.

Grewal, M.S., Andrews, A.P., 2001. Kalman Filtering: Theory and Practice, 2nd edition, John Wiley & Sons, 2001.

Hauer, A., Fumey, B., Gschwander, S., Lager, D., Lázaro, A., Rathgeber, C., Ristić, A., van Helden, W., Issayan, G. Zettl, B., 2020. Material and Component Development for Thermal Energy Storage. IEA SHC Task 58 / ECES Annex 33 IEA ECES Annex 33 - Final Report, p. 82 – 86.

Issayan, G., Zettl, B., 2021. Processing Salt-Hydrates to Thermochemical Storage Composite Materials. 15th International Virtual Conference on Energy Storage ENERSTOCK, Book of Abstracts. p. 95 – 96

Issayan, G., Zettl, B., Somitsch, W., 2021. Developing and Stabilizing Salthydrate Composites as Thermal Storage Materials. 14th International Renewable Energy Storage Conference 2020 (IRES2020) AtlantisPress, p.49-57.

Issayan, G., Zettl, B., 2022. Novel Thermogravimetric Characterization Method for Adsorption Cycles of TCM. 15th International Renewable Energy Storage Conference 2021 (IRES2021) AtlantisPress, p.108-117.

Kirchsteiger, H. and Kefer, P. “A Novel State of Charge Sensor Concept for Thermochemical Heat Storage.” 13th international conference on solar energy for buildings and industry (EUROSUN 2020), Athens, Greece, 2020.

Jin, X., Yang, W., Gao, X., Li, Z., 2020. Analysis and Modeling of the Complex Dielectric Constant of Bound Water with Application in Soil Microwave Remote Sensing, Remote Sens. 12 (2020), pp 3544

Park, C.-H., Behrendt, A., LeDrew, E., Wulfmeyer, V., 2017. New Approach for Calculating the Effective Dielectric Constant of the Moist Soil for Microwaves, Remote Sens. 9 (2017) pp 732.

Simon, D. 2006. Optimal State Estimation: Kalman, $H\infty$, and nonlinear Approaches. John Wiley & Sons, 2006.

Zettl, B., 2020. Long-term thermochemical heat storage for low temperature applications. Proceedings of the ISES Solar World Congress 2019, p. 397-402.

Zettl, B., 2022. State-of-Charge measurement techniques for PCM and TCM IEA SHC T67/ ECES Annex 40, 2nd Expert Meeting Graz, 2-4 April 2022

7 Contact

DI Dr. Bernhard Zettl
FH-OÖ F&E GmbH
4600 Wels, Stelzhamerstr. 26
Tel +43 050 804 46918
E-mail Bernhard.zettl@fh-wels.at
Website [ASiC - FH OOE (fh-ooe.at)]